ELSEVIER

Polymer 73 (2002) 6767–6773

polymer

www.elsevier.com/locate/polymer

Transport behavior of PMMA/expanded graphite nanocomposites

Wenge Zheng[a], Shing-Chung Wong[a,*], Hung-Jue Sue[b]

[a]*School of Materials Engineering, Nanyang Technological University, Nanyang Avenue, Singapore, Singapore 639798*
[b]*Polymer Technology Center, Department of Mechanical Engineering, Texas A&M University, College Station, TX 77843-3123, USA*

Received 17 June 2002; received in revised form 19 August 2002; accepted 21 August 2002

Abstract

Polymethylmethacrylate (PMMA)/expanded graphite (EG) and PMMA/untreated graphite (UG) composites were prepared by direct solution blending of PMMA with EG and UG fillers. A four-point resistivity probe system was used to measure the electrical conductivity of the composites. With the increase of filler content, the electrical conductivity of the composites showed the transition from an insulator to a semiconductor. The transition can be described by classic percolation theory with a critical exponent of 2.1 ± 0.1 for PMMA/EG and 1.8 ± 0.1 for PMMA/UG composites. Interestingly, only 0.6 vol% filler content was required to reach the percolation threshold of transition in electrical conductivity using PMMA/EG. The thickness of the EG sheet was found to be at the nanometer scale. The filler content necessary to reach the percolation threshold in PMMA/EG was found to be much lower than those required for PMMA/UG (2.0 vol% graphite) and conventional PMMA/carbon black (4.5 vol% CB) composites. Evidence was presented in this to demonstrate the improvement in electrical conductivity which was effected by the increase in filler form factor and their enhanced dispersion.

Keywords: Polymethylmethacrylate; Expanded graphite; Nanocomposite

1. Introduction

Conducting polymers have been extensively studied because of their potential applications in light emitting devices, batteries, electromagnetic shielding, anti-static and corrosion resistant coatings, and other functional applications [1–7]. To enhance the functional performance of polymers, one could consider the recent technology in reinforcement at the nanoscale [8–15]. The advantage of nanoscale reinforcement is two-fold: (1) when nanoscale fillers are finely dispersed in the matrix, the tremendous surface area developed could contribute to polymer chain confinement effects that may lead to higher glass transition temperature, stiffness and strength; and (2) nanoscale fillers provide an extraordinarily zigzag torturous diffusion path that lead to enhanced barrier performance for gas, moisture and oxygen transmissions. The latter is well studied in the nanocomposites derived from layered silicates in recent years [8–11]. Unfortunately, nanoclay reinforced polymers do not possess as good electrical conductivity, photonic and dielectric properties as some functional composites such as carbon black (CB) [1,2], metallic powder [3–5], polyaniline [6] and graphite [7] containing polymers. Among the conducting polymeric composites, one main objective in design from both economical and processing viewpoints is to minimize the filler concentration. Too high concentration of the conductive filler could lead to materials redundancy and detrimental mechanical properties [1]. In this study, we seek to develop a conducting polymer system with as small an amount of filler as possible to achieve semiconductivity.

Improvement in electrical conductivity arising from the increase of filler content was observed for most conductive composites containing CB [1,2] and metal powder [3–5]. The conductive behavior was explained by the percolation transition of the conductive network formation [1–7,16]. The transition in conductive particle containing polymers was greatly affected not only by the aggregation, structure, average size and size distribution of the second phase, but it also includes polymer rheology and processing conditions. The percolation values for critical transition are 8, 6.2, 9 and 5 wt% for PMMA/CB [16], PP/CB [17], nylon 6/CB [18] and PET/CB [19], respectively. In most cases, relatively

* Corresponding author. Present address: Department of Mechanical Engineering and Applied Mechanics, 111 Dolve Hall, North Dakota State University, Fargo, ND 58105, USA. Tel.: +1-701-231-8840; fax: +1-701-231-8913.

E-mail address: josh.wong@ndsu.nodak.edu (S.C. Wong).

0032-3861/02/$ - see front matter
PII: S0032-3861(02)00599-2

large quantities of filler were needed to reach the critical percolation value, as the particle size is at micrometer and millimeter scales. Natural graphite flakes possess good electrical conductivity (10^4 S/cm at ambient temperature) and low dielectric constant 3 at room temperature and at frequency of 1 Hz. They are layered structures with a *c*-axis lattice constant of 0.66 nm [20]. There are no reactive ion groups on the graphite layers. As a result, it is difficult to prepare the polymer/graphite nanocomposites via ion exchange reaction as commonly observed in other smectite clay nanocomposites [8–10] that intercalate the monomers or polymers into the graphite sub-layers. Nevertheless, it is understood that natural graphite flakes could be intercalated by modification with various chemical species to form the graphite intercalation compounds (GIC) [20–28]. Subjecting GIC to rapid thermal treatment produces fast volatilization of intercalant. As a result, expanded graphite (EG) is formed [21,23,27]. EG maintains the layered structures similar to natural flake graphite but with larger layer spacing [27] and higher volume expansion ratio, i.e. the ratio of the packing volume of EG to that of GIC [20–23]. Celzard et al. reported that the EG surface area was close to 40 $m^2\ g^{-1}$ and the thickness of graphite sheet was about 23 nm, calculated based on the values of packing density and specific surface area [28]. Furdin et al. reported the average sheet diameter of flat micron-sized graphite which varies from 5 to 100 μm with a sheet thickness of 100 nm as measured under SEM observation. The previous reports indicated that the graphite sheets are often less than 100 nm in thickness and the graphite filled polymers can be considered nanocomposites.

EG can be mass-produced and used in many applications such as gaskets, seals, batteries, substratum for adsorption, etc. and potential uses in depollution [23,24], medical science [25,26] and support for active carbons [29]. However, relatively little is understood of EG serving as conductive fillers in polymer–matrix composites. Celzard et al. [28] first reported the conductive behavior of 100 μm thick epoxy/EG composite films. Only 1.3 vol% EG was needed to reach the percolation threshold. The studies of Celzard showed that the EG filler on average was 10 μm in diameter and 100 nm in thickness under SEM. Recently, several authors reported that a markedly low volume fraction of EG was needed to satisfy the percolation threshold of conductivity in nylon 6/EG [30], PS/EG [31] and EG containing styrene and methylmethacrylate copolymer [32] by in situ polymerization. The reported EG filler thickness varied from 10 to 50 nm based on TEM results. In such EG-based nanocomposites, the monomers were first introduced into the pores of the EG, followed by polymerization.

EG boasts a higher volume expansion ratio than that of regular untreated graphite (UG). It has been shown that multi-pores of the EG morphology and functional acids containing OH groups will facilitate physical and chemical adsorption between the EG and polymer solution [20,24,25]. We reported the preparation of PMMA/EG composites by a solution blending method elsewhere [33]. In this paper, we emphasize the electrical transport mechanisms in UG and EG composites. Evidence will be conclusively presented in examining the effects of filler content, form factor, which is defined as the ratio of the filler equivalent diameter to the thickness of filler layer, and filler morphology on the percolation threshold of composites.

2. Experimental work

2.1. Preparation of expanded graphite

The natural flake graphite from BEISHU Graphite Company of PRC was dried at 80 °C in a vacuum oven for 24 h. It was mixed and saturated with acids consisting of concentrated sulfuric acid and concentrated nitric acid in a volume ratio of 4:1 for 24 h to form the GIC. Nitric acid serves as an oxidizer and sulfuric acid is an intercalant [21,22]. The mixture was carefully washed and filtrated with deionized water until the pH level of the solution reached 6. After being dried at 80 °C in a vacuum oven for 24 h, the GIC was rapidly expanded at 900 °C for 15 s in a muffle furnace to form EG. In order to study the filler form factor and filler morphology, acid treatment time was varied to create different form factors and filler morphology.

2.2. Preparation of PMMA/graphite composites

The PMMA/EG composites were prepared by a solution blending method. PMMA pellets were dried at 60 °C in a vacuum oven for 24 h. The dried PMMA pellets with a density of 1.2 g/cm^3 were first dissolved into solution with chloroform and then mixed with UG and EG in different weight fractions in a flask by mechanical stirring aided by a sonicator. The UG density was about 2.2 g/cm^3. The EG density was assumed to be roughly the same. This assumption is reasonable, as we only refer to the solid density of the graphite phase without including the porosity, which will be replaced by the polymer solution in the composite. The filler volume fraction was calculated from the filler weight fraction in the composites as listed in Table 1. The solvent was evaporated at 60 °C and

Table 1
Conversion of filler weight fraction to volume fraction in the EG and UG composites

Weight fraction (%)	0	0.25	0.5	0.75	1.0	2.0	3.0	5.0	10
Volume fraction (%)	0	0.13	0.28	0.41	0.56	1.1	1.7	2.8	5.6

the blends were dried at the same temperature in a vacuum oven for 24 h. The composites were hot pressed into specimens with a thickness of 500 μm for testing.

2.3. Electrical conductivity test

The conductivity of PMMA/UG and PMMA/EG composites was measured with a dispersible four-point resistivity probe system (SIGNATONE). The hot pressed sample was cut into $10 \times 4 \times 0.5$ mm^3 specimens for testing. For PMMA matrix and the composites with low filler contents, the sheet resistivity of samples was directly determined using a digital high insulation/electric leakage current meter (RP2680).

2.4. Microstructures

Scanning Electron Microscopy (SEM, Jeol-3410) was used to examine the filler shape in the composites and the filler form factor. To do so, the PMMA matrix in the composites was extracted using chloroform and separated from EG filler with a soxhlet extractor. The composite samples were first packed with filter paper and put into the soxhlet sample chamber. PMMA was completely dissolved in 200 ml chloroform, refluxed at 65 °C for 4 h. The separated filler was then transferred to a glass slide. The chloroform solvent was evaporated on a hot plate to expose EG fillers only. The filler was gold coated in an SPI sputter coater prior to SEM examination.

Photoshop 5.0 image analysis software was used to calculate the graphite sheet size based on 50–80 flat fillers from SEM micrographs. The dimensions in both selected ($d_{\parallel}$) and perpendicular ($d_{\perp}$) directions of each flat graphite sheet were measured to calculate the average sheet diameter (d) as follows:

$$d = \frac{(d_{\parallel} + d_{\perp})}{2} \tag{1}$$

The graphite sheet thickness (T) was estimated based on an average thickness of 5 graphite sheets.

As the PMMA matrix is transparent, the EG filler distribution in PMMA/EG composites from the plane and side views was directly observed using an Optical Microscope (Labophot2-Pol).

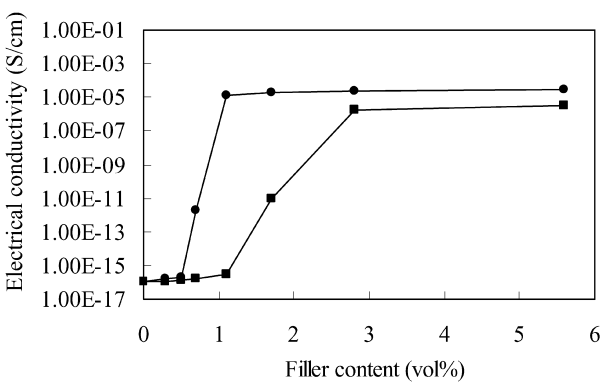

Fig. 1. Electrical conductivity of the PMMA/UG (■) and PMMA/EG (●) composites plotted as a function of filler volume fraction.

3. Results and discussion

3.1. Percolation concept

Fig. 1 shows a comparison of electrical conductivity between graphite filled PMMA with and without acid treatments. Three distinct regions could be identified on the conductivity curves. At low filler content less than 0.5 vol% for EG and 1.5 vol% for UG, the conductivity is negligible (10^{-16} S/cm) resembling that of an insulator. At slightly higher filler concentration, the composites experience a distinctive transition from low conductivity to a rapid increase in conductivity. When a percolation threshold is reached, a steady-state region occurs wherein conductivity for UG containing composites is 10^{-5} S/cm and EG composites 10^{-4} S/cm, which are consistent with that of a semiconductor. It was reported that the conductivity rose because of direct tunneling between adjacent conductive filler clusters [34,35].

According to the classical percolation theory [36,37], in the close vicinity of the percolation threshold (V_c), which corresponds to the onset of the transition from an insulator to a semiconductor, the relationship of electrical conductivity (C) of materials with filler volume fraction (V) should follow the scaling law regardless of the filler shape and distribution [36]

$$C \sim (V - V_c)^{\beta} \tag{2}$$

where β is known to be the critical exponent for percolation transition of electrical conductivity. The exponents are 2 and 1.3 for three-dimensional and two-dimensional randomly distributed objects, respectively, in the percolation model [36]. The experimental data obtained from Fig. 1 for PMMA/EG and PMMA/UG are fitted using Eq. 2 and the results are plotted in Fig. 2. Clearly, β can be estimated from

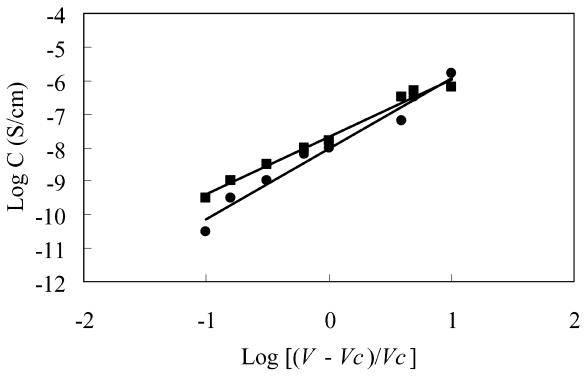

Fig. 2. Power-law dependence of the electrical conductivity (C) of the PMMA/UG (■) and PMMA/EG (●) composites as a function of the filler volume fraction (V) and critical volume fraction (V_c).

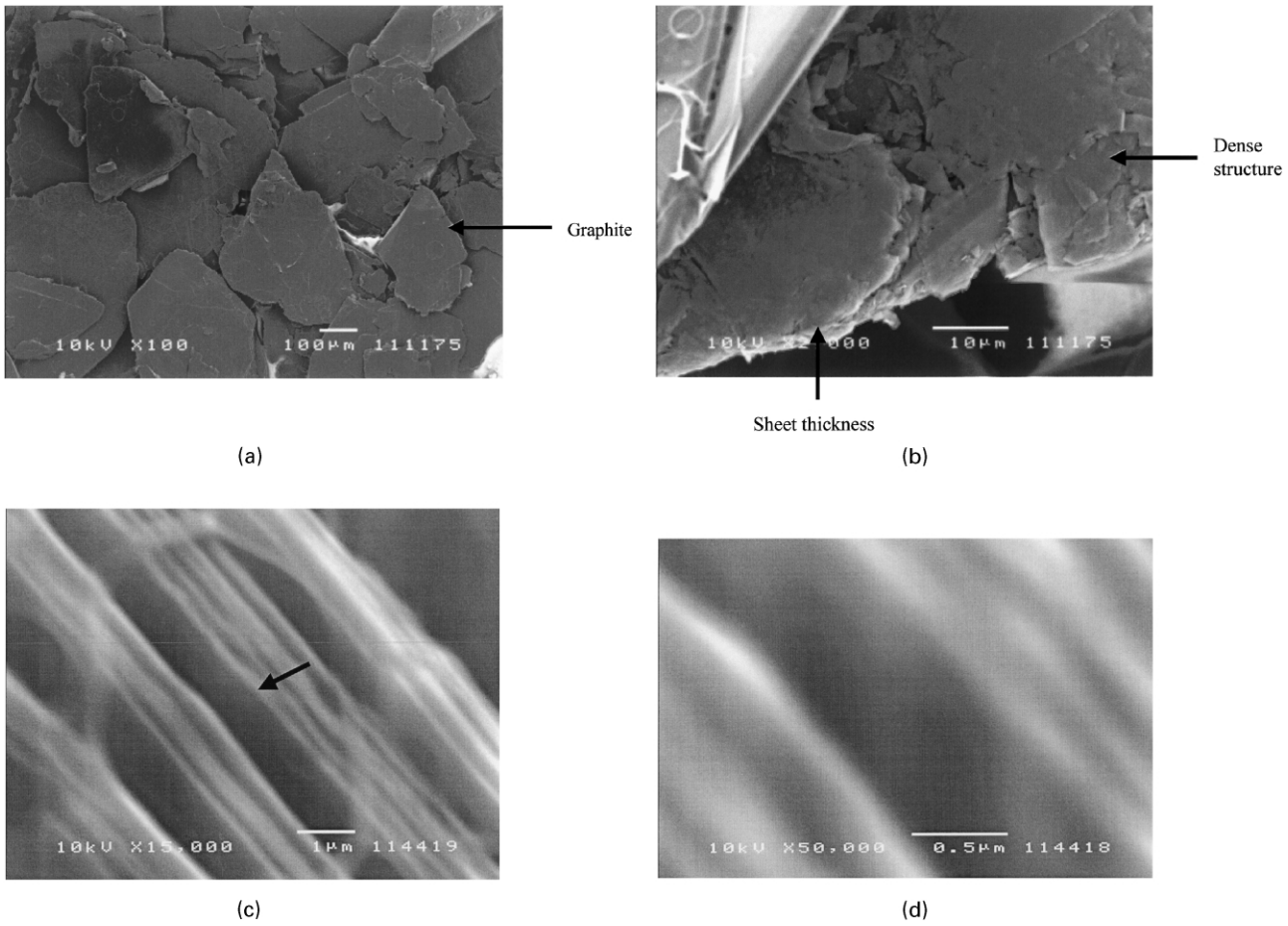

Fig. 3. SEM micrographs of (a) natural flake graphite, (b) natural flake graphite at a higher magnification, (c) expanded graphite (EG), (d) EG at a higher magnification revealing a layer thickness less than 100 nm.

the slope of the log linearity. As shown in Fig. 2, $\beta = 2.1 \pm 0.1$ and $\beta = 1.8 \pm 0.1$ for PMMA/EG and PMMA/UG composites, respectively. The compliance of the experimental data with Eq. 2 presents an indirect proof that the conductivity transition of PMMA/EG and PMMA/UG is governed by the percolation concept. The critical exponent for PMMA/UG is lower. This is attributed to the partial orientation of the graphite flake layers in the composites. Similar results were reported in PS/UG composites showing a critical exponent of 1.7 [7]

For the PMMA/UG composites, $V_c \approx 2.0$ vol%, but it reduces to $V_c \approx 0.6$ vol% when UG is replaced by EG. In other words, the EG are more effective in enhancing the electrical conductivity in PMMA than UG composites. Clearly, the EG system exhibits a markedly lower percolation threshold. In contrast, PMMA/CB conductive composites require $V_c \approx 4.5$ vol% [16]. The latter value is much higher than that for PMMA/EG. The advantage of the acid treatments on graphite for composite fabrication is evident.

Balberg et al. [38–41] reported the percolation threshold in a three-dimensional stick system. It was shown that, the percolation threshold depends on the form factor of the sticks. The percolation threshold of stick systems could be determined based on the excluded volume, which is defined as the volume around an object in which the center of another similar object is not allowed if overlapping of the two objects is to be avoided, of the sticks for non-spherical fillers. For an infinitely large system, the relationship of the critical total filler volume fraction (V_c) with filler volume (V) and excluded volume (V_{ex}) is expressed as follows [38, 41]

$$V_c = 1 - \exp\left(-\frac{KV}{V_{ex}}\right) \tag{3}$$

where K is a constant. Since K is known to be a constant in the order of 1, a small V/V_{ex} ratio means a low V_c value. In the case of PMMA/EG, we could consider the filler as randomly oriented sheets with a thickness of T and diameter d,

$$V = \pi\left(\frac{d}{2}\right)^2 \times T \tag{4}$$

and

$$V_{ex} = \pi^2\left(\frac{d}{2}\right)^3 \tag{5}$$

When $d/T \gg 1$, the percolation criterion can be given as

follows [41]

$$V_c \times f = \frac{2K}{\pi} \quad (6)$$

where f is the form factor, $f = d/T$, and K/π is a constant estimated to be about 1.

In Eq. (6), it is assumed that all fillers are of the same size. If we consider the filler size distribution in the composites, then Eq. (6) should be replaced by

$$V_c = \frac{2K}{\pi} \times [d]^2 \times \frac{T}{[d]^3} \quad (7)$$

where $[d]^3/[d]^2$ term, defined as the normalized filler diameter, is usually larger then d in Eq. (6) [40]. From Eqs. (6) and (7), it could be readily shown that, the larger the filler form factor, d/T, the lower the critical volume fraction, V_c, for conductive filler in the composites.

If we substitute $V_c \approx 0.6$ and ≈ 2.0 vol% for PMMA/EG and PMMA/UG composites, respectively, into Eq. (6), the filler form factor could be calculated to be $f = 300$ for EG filler and $f = 100$ for UG filler.

3.2. Microstructures

Fig. 3(a) and (b) shows the SEM micrographs of extracted natural flake graphite from PMMA/UG composites with filler content of 3 wt% (1.7 vol%). The average graphite sheet size estimated using an image analysis software from Fig. 3(a) is about 0.4 mm. Fig. 3(b) in higher magnification shows the graphite sheet thickness. The sheet thickness is estimated to be 5 μm, which is subject to experimental errors. Fig. 3(b) also reveals the dense structures composed of many graphite sub-layers. So the form factor of graphite filler in the composites is about 80, which is very close to 100 as calculated from Eq. (6). This supports the conclusion that relatively high form factor contributes to a markedly lower percolation threshold for PMMA/UG composites. Fig. 3(c) shows the extracted EG fillers from PMMA/EG with filler content of 2 wt% (1.1 vol%). The size of EG filler is smaller than that of UG in Fig. 3(a), as the graphite sheet was exfoliated to form smaller EG sub-layers. The average sheet size for EG is 20 μm. Fig. 3(d) shows the EG sheet in higher magnification. The average EG sheet thickness is about 50–100 nm, which agrees with the value by Furdin et al. [29]. So the EG fillers had the higher form factor of about 200–400, which is quite close to the calculated value of 300 using Eq. (6). Fig. 4 shows a schematic illustration of filler morphological effect on the percolation threshold of the composites. The conductivity of the composites is determined by the contact of conductive fillers. When the filler content is low, the probability for graphite (UG) to be in contact is small. However, when the graphite is well exfoliated into nanoscale EG layers, the number and the aspect ratio of the graphite sheets are greatly increased. Thus, the probability of forming a conducting network is also greatly enhanced, which leads to a low percolation threshold.

It is understood that EG dispersion and orientation are important parameters for the percolation threshold for transition of conductivity in the composites. In this experiment, we applied intensive stirring and employed ultrasonic bath to promote optimal dispersion for the graphite in composites. Sufficient adsorption between the PMMA molecular chains and pores of the EG strongly contributes to the good dispersion. Fig. 5(a) and (b) shows the TOM micrographs of the PMMA/EG composites from the plane and side views. EG can be considered as in three-dimensional random distribution.

3.3. Effect of acid treatment time

To investigate the effects of acid treatment, thereby filler excluded volume and form factor on the percolation threshold of PMMA/graphite composites, an experiment was designed to keep the filler content constant at 2 wt% (1.1 vol%). However, the acid treatment time for EG was varied. Fig. 6 shows the electrical conductivity of the composite as a function of acid treatment time. With the increase of acid treatment time from 0 to 120 min, the electrical conductivity of the composites increases from that pertaining to an insulator to one of a semiconductor. The transition can be attributed to the changes in acid treatment time, which would lead to the change in excluded volume for the fillers in the composites from Eq. (3). The critical form factor calculated using Eq. (6) was about 200 for the percolation threshold based on the filler volume fraction of 1.1 vol%.

Fig. 7 shows the filler SEM micrographs under different acid treatment times. The PMMA matrix was extracted from all the investigated composites by soxhlet extraction with chloroform solvent to expose only EG filler for SEM observation.

At low acid treatment time (5 min), Fig. 7(a) shows some EG structures and unexpanded graphite coexisted in the filler. In this case, the expanded structure has smaller volume expansion ratio and smaller specific surface area

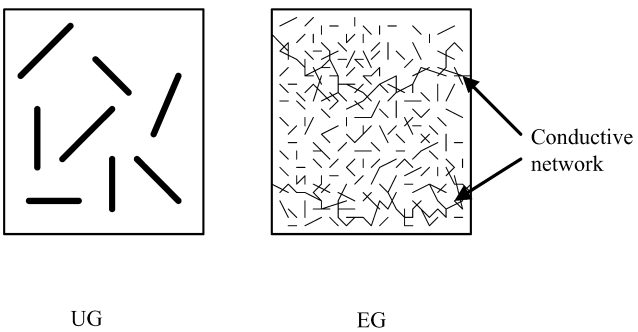

Fig. 4. 2D Schematic illustration of different filler morphology effect on the conductive network formation in PMMA/UG and PMMA/EG composites at a low filler content, the solid line represents the graphite sheets and EG sheets, respectively, viewed from the direction parallel to the filler sheets.

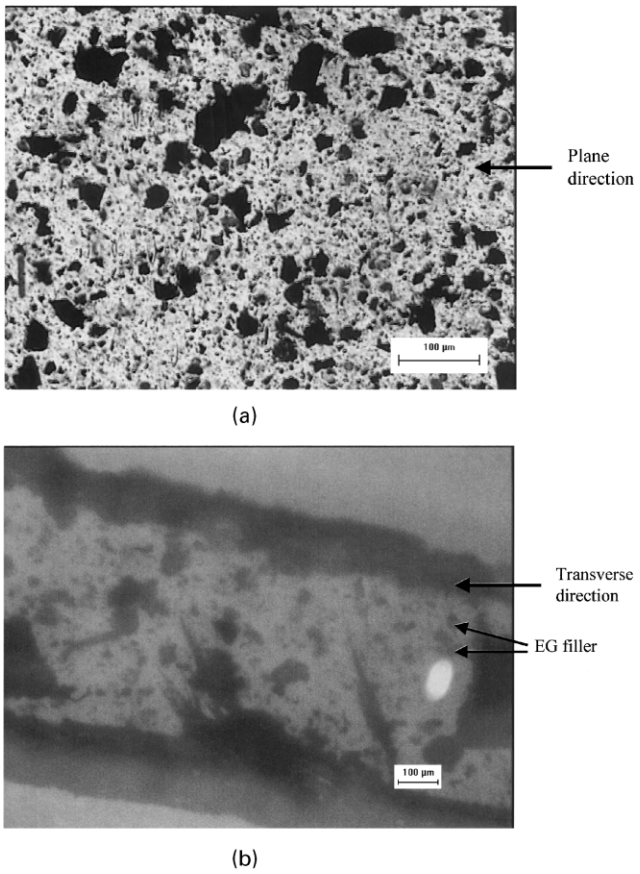

Fig. 5. Optical micrographs of PMMA/EG composites with 1.1 vol% EG from (a) plane view, (b) side view perpendicular to the plane view, the dark phase is EG filler.

than that of completely expanded graphite. So, the increase of the conductivity was only due to the increase of the filler excluded volume (V_{ex}) from EG structure in Eq. 3.

With longer acid treatment time (15 min), Fig. 7(b) indicates that all the graphite sheets were expanded to form the expanded structure with larger volume expansion ratio and specific surface area. Fig. 6 revealed the sharp increase in the electrical conductivity of the composites due to the acid treatment time. Physically, the increase may be

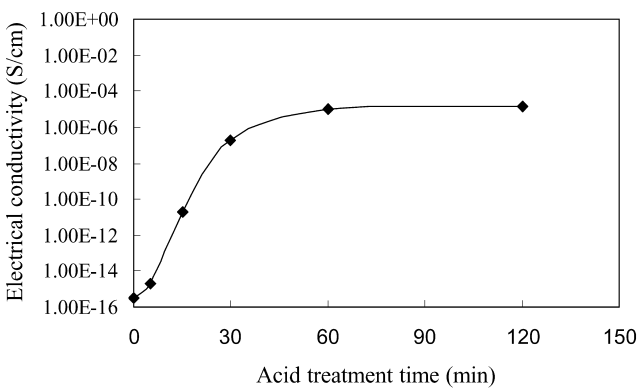

Fig. 6. The electrical conductivity of PMMA/EG vs the acid treatment time.

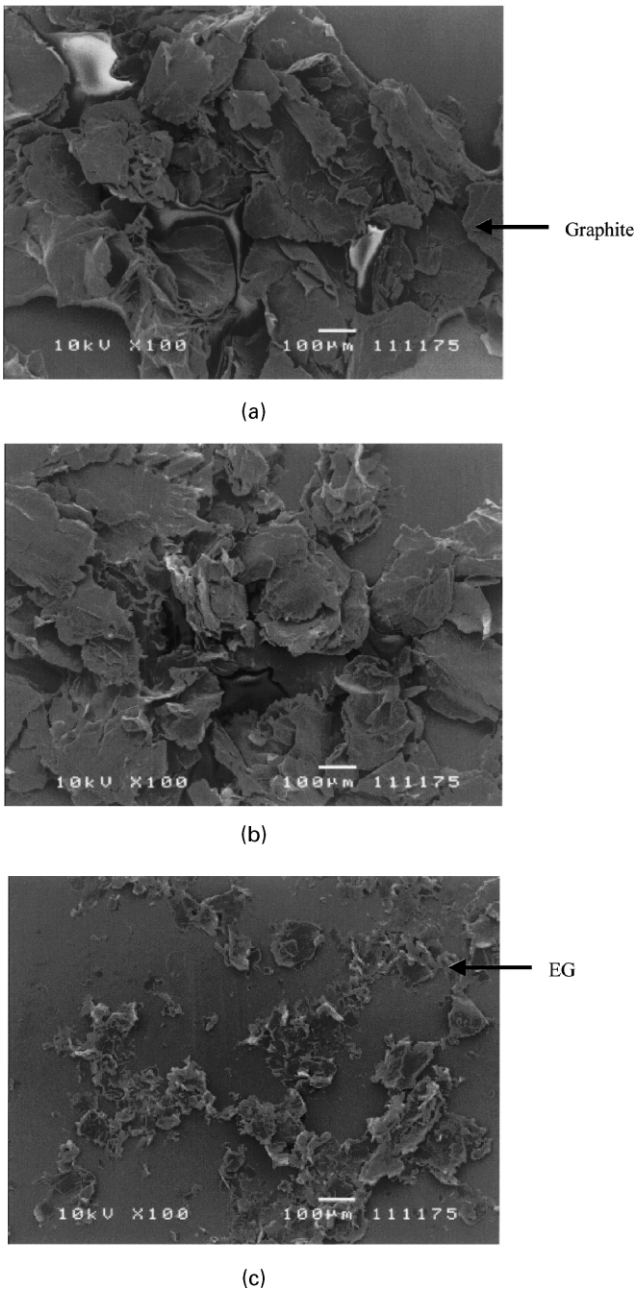

Fig. 7. SEM micrographs of EG from the PMMA/EG composites with different acid treatment time: (a) 5 min, (b) 15 min and (c) 60 min.

attributed to the rapid increase of the excluded volume of fillers.

With prolonged acid treatment time (60 min), Fig. 7(c) revealed similar EG filler morphology to that in Fig. 3(c), which is obtained from EG alone. The graphite sheets were completely expanded and split into small pieces of EG filler with the form factor of about 200–400. At this stage, the composite has higher electrical conductivity as evidenced in Fig. 6. The filler morphological characteristics indicate that the electrical conductivity of composites is greatly influenced by filler morphology.

4. Conclusions

The electrical transport properties of PMMA/EG and PMMA/UG composites were studied and the following conclusions could be drawn:

1. With the increase of filler content, the electrical conductivity of the PMMA/EG and PMMA/UG composites showed a transition from an insulator to a semiconductor.
2. The transition could be described by classical percolation theory with a critical exponent of 2.1 ± 0.1 for PMMA/EG and 1.8 ± 0.1 for PMMA/UG composites.
3. The PMMA/EG nanocomposites exhibited the lowest percolation threshold ($V_c = 0.6$ vol%) in comparison to the PMMA/UG composites (2.0 vol%) and the conventional PMMA/CB conductive composites (4.5 vol%). The improvement of percolation threshold in the composites was attributed to the increased filler form factor in EG composites.
4. With an increase in acid treatment time, the composites showed pronounced propensity for conductivity transition from an insulator to a semiconductor.
5. The filler content, filler form factor, acid treatment time and morphology appeared to be among the important parameters governing the electrical conductivity of PMMA/EG composites.

References

[1] Sichel EK. Carbon black-polymer composites. New York: Marcel Dekker; 1982.
[2] Ishigure Y, Iijima S, Ito H, Ota T, Unuma H, Takahashi M, Hikichi Y, Suzuki HJ. Mater Sci 1999;34:2979–85.
[3] Pinto G, Jimenez-Martin A. Polym Compos 2001;22:65–70.
[4] Roldughin VI, Vysotskii VV. Prog Org Coat 2000;39:81–100.
[5] Flandin L, Bidan G, Brechet Y, Cavaille JY. Polym Compos 2000;21:165–74.
[6] Ray SS, Biswas M. Synth Met 2000;108:231–6.
[7] Quivy A, Deltour R, Jansen AGM, Wyder P. Phys Rev B 1989;39:1025–9.
[8] Alexandre M, Dubois P. Mater Sci Engng 2000;R28:1–59.
[9] Usuki A, Kojima Y, Kawasumi M, Okada A, Fukushima Y, Kurauchi T, Kamigaito O. J Mater Res 1993;8:1179–83.
[10] Theng BKG. The chemistry of clay-organic reactions. New York: Wiley; 1974.
[11] Lagaly G. Appl Clay Sci 1999;15:1–9.
[12] Jana SC, Jain S. Polymer 2001;42:6897–905.
[13] Saujanya C, Radhakrishnan S. Polymer 2001;42:6723–31.
[14] Calvert P. Potential applications of nanotubes. In: Ebbesen TW, editor. Carbon nanotubes. Boca Raton, FL: CRC press; 1997.
[15] Favier V, Canova GR, Shrivastava SC, Cavaille JY. Polym Engng Sci 1997;37:1732–9.
[16] Zois H, Apekis L, Omastova M. Proceedings—International Symposium on Electrets. 10th International Symposium on Electrets (ISE 10); 1999. p. 529–32.
[17] Mamunya EP, Davidenko VV, Lebedev EV. Compos Int 1997;4:169–76.
[18] Gabriel P, Cipriano LG, Ana JM. Polym Compos 1999;20:804–8.
[19] Mallette JG, Marquez A, Manero O, Castro-Rodriguez R. Polym Engng Sci 2000;40:2272–8.
[20] Dresselhaus MS, Kalish R. Ion implantation in diamond, graphite and related materials. Berlin: Springer; 1992.
[21] Chung DDL. J Mater Sci 1987;22:4190–8.
[22] Cao NZ, Shen WC, Wen SZ, Liu YJ, Wang ZD, Inagaki M. Mater Sci Engng (Chinese) 1996;14:22–6.
[23] Tryba B, Kalenczuk RJ, Kang FY, Inagaki M, Morawski AW. Molecular crystals and liquid crystals science and technology. Section A. Molecular crystals and liquid crystals, vol. 340. ISIC 10—10th International symposium on intercalation compounds; 2000. p. 113–9.
[24] Toyoda M, Inagaki M. Carbon 2000;38:199–210.
[25] Liu JP, Song KM. J Funct Mater (Chinese) 1998;29:659–61.
[26] Cao N, Shen W, Wen S, Liu Y. Chem Bull 1996;4:37–41.
[27] Celzard A, Mareche JF, Furdin G, Puricelli S. J Phys D: Appl Phys 2000;33:3094–101.
[28] Celzard A, McRae E, Mareche JF, Furdin G, Dufort M, Deleuze C. J Phys Chem Solids 1996;57:715–8.
[29] Furdin G, Marceche JF, Herold A. French Patent, FR2682370; 1993.
[30] Pan YX, Yu ZZ, Ou YC, Hu GH. J Polym Sci, Part B: Polym Phys 2000;38:1626–33.
[31] Xiao P, Sun L, Xiao M, Gong K. Mater Res Soc Symp Proc, Boston 2001;661:KK531–6.
[32] Chen GH, Wu DJ, Weng WG, Yan WL. J Appl Polym Sci 2001;82:2506–13.
[33] Zheng WG, Wong SC. Electrical and dielectric properties of PMMA/expanded graphite composites. Compos Sci Tech 2002; in press.
[34] Van der Putten D, Moonen JT, Brom HB, Brokken-Zijp JCM, Michels MA. Phys Rev Lett 1992;69:494–7.
[35] Calberg C, Blacher S, Gubbeis F, Brouers F, Deltour R, Jerome R. J Phys D: Appl Phys 1999;32:1517–25.
[36] Stauffer D, Aharony A. Introduction to percolation theory. London: Taylor & Francis; 1991.
[37] Grimmett G. Percolation. New York: Springer; 1989.
[38] Balberg I, Anderson CH, Alexander S, Wagner N. Phys Rev B 1984;30:3933–44.
[39] Balberg I, Binenbaum N, Wagner N. Phys Rev Lett 1984;52:1465–7.
[40] Balberg I. Phys Rev B 1985;31:4053–5.
[41] Balberg I. Phys Rev B 1986;33:3618–20.